MAGMA (2005) 18: 7–18
DOI 10.1007/s10334-004-0073-5

RESEARCH ARTICLE

M. G. Danilouchkine
J. J. M. Westenberg
J. H. C. Reiber
B. P. F. Lelieveldt

Accuracy of short-axis cardiac MRI automatically derived from scout acquisitions in free-breathing and breath-holding modes

Received: 28 May 2004
Revised: 5 August 2004
Accepted: 7 September 2004
Published online: 28 January 2005

M. G. Danilouchkine · J. J. M. Westenberg
B. P. F. Lelieveldt · J. H. C. Reiber
Div. Image Processing,
Dept. Radiology, Bld.1 C2S-C3Q50,
Leiden University Medical Center,
P.O.Box 9600, 2300RC Leiden,
The Netherlands
E-mail: M.G.Danilouchkine@lumc.nl
Tel.: +31-71-5261117
Fax: +31-71-5266801

Abstract To qualitatively assess the accuracy of automated cardiovascular magnetic resonance planning procedures devised from scout acquisitions in free-breathing and breath-holding modes, to quantitatively evaluate the accuracy of the derived left ventricular volumes, mass and function and compare these parameters with the ones obtained from the manually planned acquisitions. Ten healthy volunteers underwent cardiovascular MR (CMR) acquisitions for ventricular function assessment. Short-axis data sets of the left ventricle (LV) were manually planned and generated twice in an automatic fashion. Automated planning parameters were derived from gated scout acquisitions in free-breathing and breath-holding modes. End-diastolic volume (EDV), end-systolic volume (ESV), ejection fraction (EF), and left ventricular mass (LVM) were measured. The agreement between the manual and automatic planning methods, as well as the variability of the aforementioned measurements were assessed. The differences between two automated planning methods were also compared. The mean differences between the manual and automated CMR planning derived from gated scouts in free-breathing mode were 8.05 ml (EDV), 1.84 ml (ESV), 0.69% (EF), and 4.72 g (LVM). The comparison between manual and automated CMR planning derived from gated scouts in breath-holding mode yielded the following differences: 4.22 ml (EDV), 0.34 ml (ESV), 0.3% (EF), and −0.72 mg (LVM). The variability coefficients were 3.72 and 3.66 (EDV), 5.6 and 8.19 (ESV), 3.46 and 4.31 (EF), 6.49 and 5.20 (LVM) for the automated CMR planning methods derived from scouts in free-breathing and breath-holding modes, respectively. Automated CMR planning methods can provide accurate measurements of LV dimensions in normal subjects, and therefore may be utilized in the clinical environment to provide a cost-effective solution for functional assessment of the human cardiovascular system.

Introduction

Understanding and consequent treatment of cardiovascular diseases relies substantially on the accurate assessment of cardiac volume, mass, and function [1,2]. The most widely available tool to carry out such an assessment is two-dimensional echocardiography. While the image acquisition has proven to be highly reproducible in normal individuals, the quantitative analysis is restricted by the geometric assumptions imposed on the shape of the human heart in these two-dimensional images [3,11,12]. An alternative technique to echocardiography

is cardiovascular magnetic resonance (CMR) imaging, which is free from any geometric assumptions because of its truly three-dimensional characteristics and has been proven to be accurate [4,5,20] and reproducible [6,7,21].

In spite of these apparent advantages, the widespread utilization of CMR in clinical practice is mainly confined by two factors, namely high hospital costs from the use of CMR and increased examination time, which cannot be well tolerated by all patients. Both factors partially originate from the complexity of the CMR planning procedure, but their impact can be significantly reduced. In order to make CMR a more cost-effective technology, automated image analysis techniques can provide new possibilities to radiologists and radiographers.

A first step involves careful planning of MRI acquisitions. The human heart anatomy is relatively complex, and appearance of the cardiac structures depends on the spatial position of the imaging plane. The most useful imaging planes are those perpendicular to the LV cardiac axes, commonly known as the short-axis (SA) view [13,23,24]. Definition of the correct location and orientation of the SA imaging planes requires preliminary scout images, two additional acquisitions in long-axis directions or so-called two-chamber (2chv) and four-chamber (4chv) views [13,23,24], as well as good understanding of the target anatomy. Moreover, the radiographer is presented with the results of the intermediate acquisitions, which are two-dimensional in nature. Hence, the planning of the anatomy with the nontrivial spatial orientation and geometry becomes a time-consuming, labor-intensive and knowledge-specific task.

The complexity of CMR planning also requires use of standardized acquisitions. Although modern MRI scanners come with the predefined set of cardiac scanning protocols, the latter are independent of geometric assumptions. Therefore each patient's imaging session must be tailored to accommodate individual variations of the heart spatial orientation. In spite of the fact that use of a protocol may facilitate and accelerate the planning procedure, this task remains a challenging job even for experienced radiologists.

In our laboratory we developed a novel system [9, 16,17] that enables us to automate the procedure of SA acquisition planning. Our approach is based upon a geometric model of the human thorax. This model describes the shapes of thoracic organs with the distinct air-tissue boundaries. The feature points obtained by automatic segmentation of the lung and thorax surfaces in scout acquisitions are registered against the geometric model. Once the feature points are aligned with the model, the orientation of the LV axis can be computed and the imaging planes for SA acquisitions can be devised.

One of the original contributions of this paper is to qualitatively assess the accuracy of automated CMR planning and to compare this with manual planning, as well as to quantitatively evaluate the accuracy and variability of the cardiac volumes, mass and function. The accuracy of the automated technique is of crucial importance in establishing its clinical feasibility and potential applicability in a hospital environment. This factor comprises the minimal requirement imposed on all computer-aided diagnostic tools and provides an answer to the question of whether the manual and automatic methods can be used interchangeably in everyday clinical practice.

A second original contribution is to compare two automated CMR planning procedures: one derived from the gated in free-breathing mode and the other one from the gated scouts in breath-holding mode. The scouts are commonly used to locate the global position of the heart within the thoracic cavity and are usually acquired in non-gated mode without respiratory or electrocardiographic (ECG) triggering. Segmentation of non-gated scouts results in a noisy set of feature points, which may negatively affect the accuracy of automated CMR planning. To improve this situation, modified versions of the scout acquisitions were proposed. Both scouts were acquired with ECG triggering. One version of scouts was obtained in free-breathing mode, while the other was obtained in breath-holding mode. The accuracy of automated CMR planning methods derived from gated scouts in free-breathing and breath-holding modes is assessed. Furthermore, the accuracy of cardiac volumes, mass and function measurements obtained from both automated planning methods is compared with the manually planned acquisitions.

Materials and methods

Patient population

Ten healthy volunteers (eight men and two women; mean age 30 ± 5; age range 23–38) underwent the CMR imaging procedures. All subjects enrolled in the study had neither a history of cardiac diseases nor identified risk factors. The study was carried out in accordance with the institutional regulations and was approved by the ethics committee. Prior to examination all subjects gave informed written consent.

Image acquisition

MR imaging was performed with a Philips Gyroscan Intera 1.5-T scanner (Philips Medical Systems, Best, The Netherlands) using a dedicated five-element synergy cardiac coil and prospective ECG triggering.

Protocol for manual CMR planning

For manual CMR planning, the conventional clinical protocol [18,19] used in our institution was adhered to. An operator with

extensive experience in CMR planning carried out the manual planning. Imaging consisted of acquisitions of balanced-FFE scout images, and subsequent two- and four-chamber cinematic (cine) images. A stack of breath-hold short-axis cine cross sections was acquired from the apex to the mitral valve with an 8.0-mm slice thickness and 2.0-mm slice gap. Each cross section was acquired in a separate breath-hold at end expiration. The number of reconstructed cardiac phases was set to 30, 8–13 slices were acquired to completely encompass the LV from the apex up to the atrioventricular ring. Segmented steady-state free-precession breath-hold cines (Balanced-FFE) were used for all slices and acquisitions with the following parameters: TR-2.3 ms and TE-1.25 ms (scout acquisitions); TR-3.0 ms and TE-1.56 ms (2chv); TR-3.3 ms and TE-1.63 ms (4chv); TR-3.1 ms and TE-1.55 ms (SA acquisitions); slice thickness 8 mm, slice gap 2 mm, field of view 45 × 45 cm (scouts) and 35 × 35 cm (other), acquisition matrix 128 × 128 (scouts) and 192 × 192 (other), reconstruction matrix 256 × 256, number of frames 30 with the average temporal resolution of 20–25 ms depending on the heart rate, and flip angle 50°. The R-wave was used as a trigger to perform prospective ECG gating.

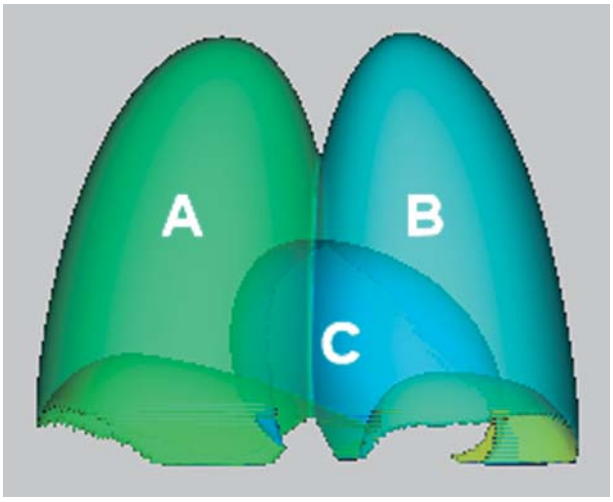

Fig. 1 Three-dimensional geometric model of the human thorax includes the following anatomical organs: right lung (A) and left lung (B). The cavity in between the lungs (C) describes the boundary between the heart and the lungs

Protocol for automated CMR planning

A novel system for automated CMR planning was developed in our laboratory and described in previous publications [9, 16, 17]. It is based upon a three-dimensional geometric model of the human thoracic cavity. This model describes the shapes of thoracic organs with the profoundly distinct air-tissue boundaries such as lungs, heart, spleen, liver etc. (Fig. 1). To account for variability in shapes, location and spatial orientation of the organs, the correspondence between the modeled organs and the scanned thoracic data has to be established. To achieve this, the scout images of the examined subject are automatically segmented, resulting in a set of three-dimensional feature points. Consequently, these feature points are aligned with the geometric model in such a way that the maximal correspondence between the subject's specific data and the model is achieved (Fig. 2). Thus the aforementioned organs in the scan data of the examined subject are recognized and the spatial location and orientation of the modeled heart can be projected back from the model coordinate system into the imaging domain. Knowing the exact location and orientation of the heart inside the subject's thoracic cavity, the imaging planes for SA acquisitions can be devised.

The experimental setup for automated CMR planning includes the scanner and the remote workstation connected to one another via the network. The acquired scout images were transferred via the DICOM protocol from the scanner to the workstation running the proprietary software. The program automatically segments the input images, extracts a set of the feature points, establishes the correspondence between the model of the human thorax and the scanned data of the examined subject, and computes the spatial location and orientation of the subject's heart in the coordinate system of the scanner. The suggested location and orientation of the SA imaging planes are manually transferred to the operator's console of the scanner. The number of slices was chosen by the operator to assure complete coverage of the left ventricle from the apex to the atrioventricular ring.

Automated planning of SA acquisitions was devised for each subject twice from two different scouts. In our first experiment, the modified scouts were used: multiple slice (15 transversal, 15 coronal, and 15 sagittal images) turbo field-echo pulse protocol (turbo factor 64 and linear profile order), performed in free-breathing mode with ECG triggering and the R-peak of the ECG as a trigger, applied with the following parameters: TR-6.9 ms and TE-3.5 ms; slice thickness 8 mm and a 2 mm slice gap, field of view 45 × 45 cm, acquisition matrix 256 × 256, reconstruction matrix 256 × 256, and flip angle 20°. However, segmentation of gated scouts in free-breathing mode results in a noisy set of feature points due to respiratory artifacts. This factor potentially has a negative influence on the automatic estimations of the LV axis orientation and may introduce a tilt and/or displacement in the orientation of the SA imaging planes. To eliminate these artifacts and increase the accuracy of automated planning a modified version of the scout acquisition was adopted in our second experiment. The multiple slice (10 transversal and 10 sagittal images) turbo field-echo pulse protocol (turbo factor 64 and linear profile order) was performed at end-expiration with the following parameters: TR-6.9 ms and TE-3.5 ms; slice thickness 10 mm, slice gap 4 mm, field of view 45 × 45 cm, acquisition matrix 256 × 256, reconstruction matrix 192 × 192, and flip angle 20°. The R-wave was again used as a trigger to perform prospective ECG gating.

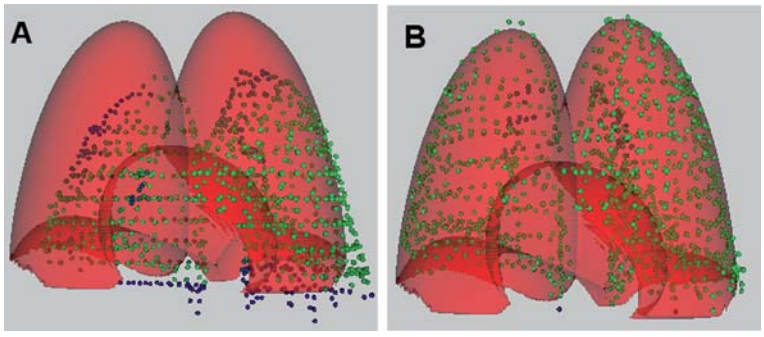

Fig. 2 The feature points (*green and blue*) extracted from the scouts of the examined patient and describing the air-tissue boundaries in the thoracic cavity. The maximal correspondence between the geometric model (*red*) and the feature points is achieved during the alignment procedure (feature points and model before (*A*) and after (*B*) matching)

Image analysis

Analysis was performed with a personal computer using the MASS software (Medis medical imaging systems bv, Leiden, the Netherlands) and done by one experienced observer in accordance with the general guidelines for image analysis [14]. Prior to the analysis the acquired data sets were anonymized and presented in random order to the observer. The first cine phase of each SA acquisition corresponded to end-diastole due to the prospective ECG triggering. The cine movie for a mid-ventricular slice was observed to identify end-systole as the phase with the minimal area of the LV blood pool. Due to the heart rate variability, the end-systolic phase was independently detected for each SA acquisition. The epicardial and endocardial LV borders were manually outlined in both end-diastole and end-systole. The contours were delineated in all slices where the myocardium exposed at least half of its circumferential length [14, 22]. Due to the fact that the endocardial border identification is difficult, especially in the apical slice at the end-systolic phase, we adhered to a strict set of guidelines. The papillary muscles and trabeculations were disregarded in the manual segmentation and were assigned to the LV blood pool. The RV trabeculations appearing as pouches along the septal wall and subepicardial fat were excluded from LV mass. Summation over the volume of each individual short-axis slice was used to quantify the end-diastolic and end-systolic volumes (Simpson rule). The weighted difference between the epicardial and endocardial volumes comprises the LV mass. The commonly used density factor of 1.05 g/cm^3 served as the weighting coefficient in the calculation of the LV mass.

Visual analysis of accuracy

To assess the accuracy of CMR planning a system of visual scores was adopted. This system was based upon the observer's judgment. The automatic SA imaging planes were projected back into 2chv and 4chv and the LV axis deviation was visually classified into three categories: excellent (perfect alignment), acceptable (the automatic LV axis was slightly deviated) and unacceptable (the deviation was more than 7–8°). The automatic planning was considered to be excellent when the LV axis deviations in both views had the excellent scores, to be acceptable when the score was acceptable in one projection and excellent in the other (Fig. 3). The rest of the cases were considered unacceptable.

Quantitative analysis of accuracy

To evaluate quantitatively the accuracy of CMR planning the following approach was used. The spatial orientation of the imaging plane of the manual SA series was chosen as the reference. The angular difference between the reference and the orientation of the imaging plane of another SA acquisition was used to characterize the planning accuracy. The mean values as well as the standard deviations of the angular differences were calculated for other SA acquisitions resulting in quantitative measurements of the accuracy of the automated CMR planning procedures.

LV function analysis

The calculated functional parameters were statistically analyzed. Firstly, the Pearson correlation coefficient was computed to estimate the strength and direction of a linear relationship between two measurements. Secondly, the paired t-test was employed to find out the statistical significance of the differences between the functional parameters. The level of statistical significance was established at 0.05. Thirdly, the Bland–Altman analysis [8] was performed to quantify the agreement between different methods. Finally, the degree of variability (expressed as a percentage) was assumed to be the standard deviation of the differences between two measurements with respect to their mean value [4, 7, 14].

Results

All subjects included in the study tolerated CMR well. The total imaging time did not exceed 45 min. All subjects had

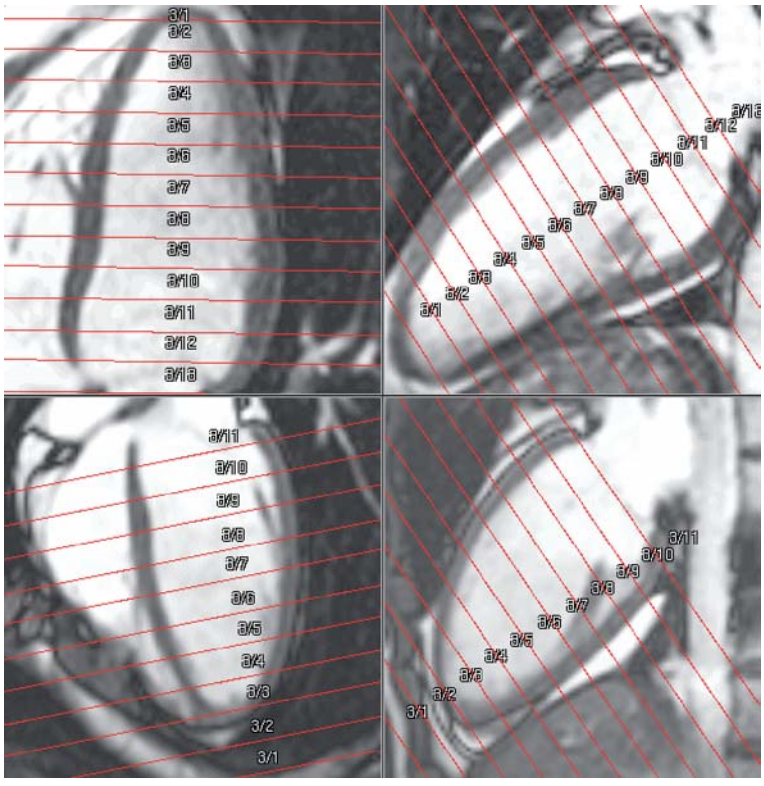

Fig. 3 Projection of the short-axis imaging planes (*red lines*) into two- and four-chamber views. Two top images present an example of the excellent visual score. The imaging planes are perpendicular to the left ventricular axis in both projections. The automated planning on the bottom provides an example of the unacceptable visual score because the short-axis imaging planes are slightly angled in both projections

normal sinus rhythm. The average breath-hold time for a cine acquisition was between 15 and 17 s, tolerated well by all subjects and allowing up to 30 phases per cardiac cycle to be acquired.

Image and contour comparison

The acquired SA images had sufficient quality and high contrast between the blood and myocardium to outline the contours. The examples of manually planned and automatically devised SA acquisitions at end-diastole are shown in Fig. 4. The SA cross sections for both type of planning procedures have similar appearance. Fig. 5 shows the manually delineated contours for the same subject.

Ventricular volume, ejection fraction and mass quantification

The results of the statistical analysis for end-diastolic volume (EDV), end-systolic volume (ESV), ejection fraction (EF), and left ventricular mass (LVM) are summarized in Table 1 and 2. The mean values of these parameters were not significantly different for both automated planning methods, with the exception of the EDV and LVM parameters for automated CMR planning derived from gated scouts in free-breathing mode and the EDV parameter for automated CMR planning derived from gated scouts in breath-holding mode. All parameters demonstrated the consistently high degree (> 97%) of correlation between manual planning and the automated planning methods, but for EF that turned out to be 86% and 84% for automated CMR planning derived from scouts in free-breathing and breath-holding modes, respectively. In general, the variability coefficients were low (< 9°), showing a good agreement of CMR measurements between

Table 1 CMR measurements [mean ± SD for *EDV* – end-diastolic volume, *ESV* – end-systolic volume, *EF* – ejection fraction, *LVM* – LV mass]

	EDV (ml)	ESV (ml)	EF (%)	LVM (g)
Manual	185 ± 38	70 ± 16	62 ± 4	133 ± 31
Auto in Free-breathing	177 ± 38	68 ± 17	62 ± 4	129 ± 33
Auto with Breath-holding	181 ± 36	69 ± 19	62 ± 5	134 ± 32

Calculated from manually planned short-axis acquisitions and from automatically planned short-axis acquisitions derived from scouts in free-breathing mode and with breath-holding

Table 2 Comparison of CMR measurements for the automatically planned short-axis acquisitions derived from gated scouts in free-breathing and breath-holding modes with those from manual planning

	EDV (ml)	ESV (ml)	EF (%)	LVM (g)
Man. versus free-breathing auto				
Mean diff. ± SD	8.05 ± 6.43	1.84 ± 3.6	0.69 ± 2.18	4.72 ± 6.3
Corr. coeff.	0.99	0.98	0.86	0.98
t-test (*P*-value)	0.02(S)	0.07(Ns)	0.17(Ns)	0.02(S)
Variability coefficients	3.72	5.6	3.46	6.49
BA limits	−4.56:20.66	−5.23:8.9	−3.59:4.96	−7.44:16.87
Man. versus breath-holding auto				
Mean diff. ± SD	4.22 ± 6.64	0.34 ± 5.02	0.3 ± 2.73	−0.72 ± 7.02
Corr. coeff.	0.98	0.97	0.84	0.98
t-test (*P*-value)	0.04(S)	0.42(Ns)	0.37(Ns)	0.38(Ns)
Variability coefficients	3.66	8.19	4.31	5.2
BA limits	−8.8:17.23	−9.5:10.17	−5.05:5.64	−14.48:13.04

EDV – end-diastolic volume, *ESV* – end-systolic volume, *EF* – ejection fraction, *LVM* – left ventricular mass at end-diastole, *Mean diff.* – mean difference (manual-auto), *Corr. coeff.* – correlation coefficient, *BA limits* – Bland–Altman limits of agreement, *S* – significant difference, *Ns* – non-significant

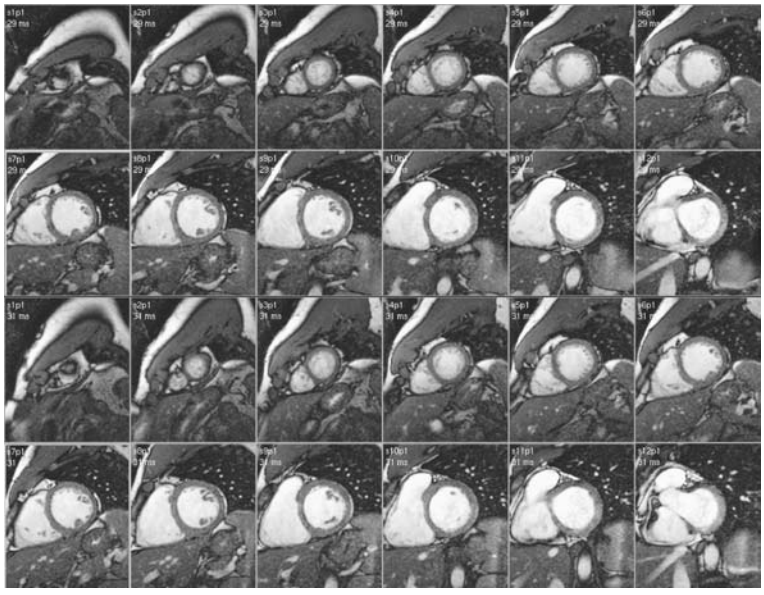

Fig. 4 Short-axis cross sections for manual (*two top rows*) and automated (*two bottom rows*) CMR planning methods. Although the sections are shifted with respect to each other along the direction of the LV axis, their appearance is similar for both methods of CMR planning

the manual and automated planning methods. The paired t-test comparing two automated methods with each other revealed no significant differences between the ESV and EF variability coefficients. The EDV and LVM variability coefficients appeared to be statistically significant (*P*-values 0.03 and 0.02 respectively) favoring the automated planning derived from the gated scouts in breath-holding mode (Fig. 6). The calculated Bland–Altman limits of agreements emphasize the strength of the relation between measurements and are given in Fig. 7. The plots showed no systematic bias in differences between measurements with respect to their means, and in general the limits of agreement for measurements for both automated planning methods had comparable ranges.

Visual scores

For the automated planning derived from gated scouts in free-breathing mode the excellent score was achieved for four subjects, acceptable—for three subjects, and unacceptable—for the remaining three subjects. For the automated planning derived from gated scouts in breath-holding mode the unacceptable scores dropped to two

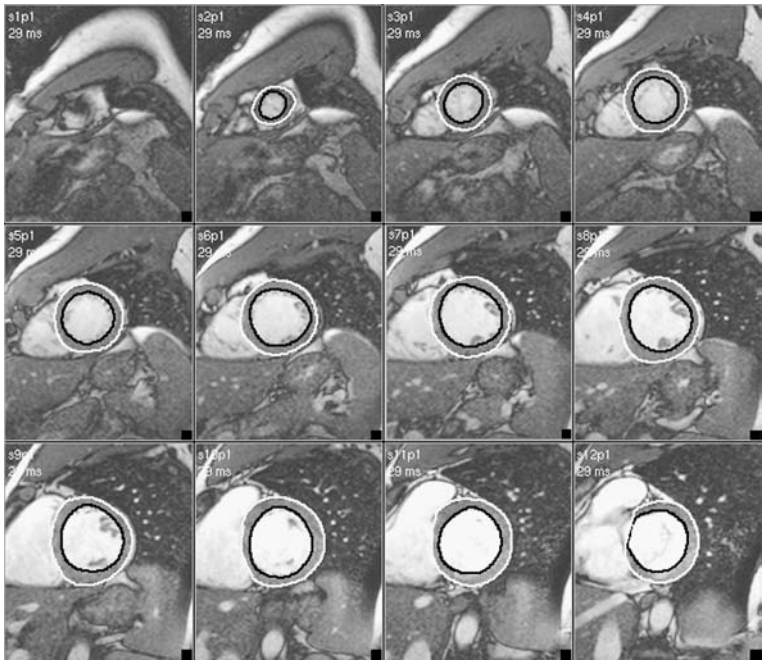

Fig. 5 Endocardial (*black*) and epicardial (*white*) contours manually delineated for the same subject

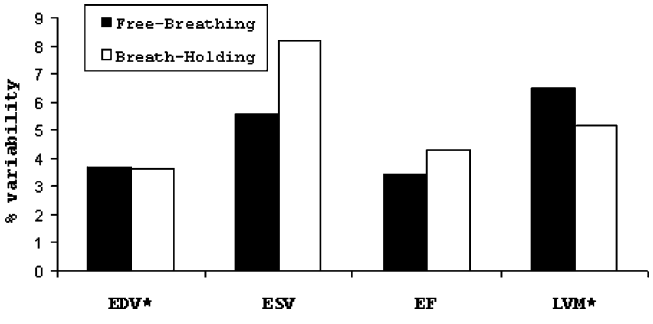

Fig. 6 Bar chart for variability coefficients (expressed as a percentage and equal to the standard deviation of the differences between two measurements divide by the their mean) of CMR measurements derived from scouts in free-breathing and breath-holding modes versus ones derived from the manual planning. The * emphasizes the statistically significant difference between the two methods of automated CMR planning

cases in favor of one extra acceptable score. The number of excellent scores remained the same.

LV axis deviation

The mean and standard deviation of the LV axis were 7.77 ± 5.36 and 7.13 ± 3.64 for automated CMR planning methods derived from gated scouts in free-breathing and breath-holding modes, respectively. According to this criterion, automated CMR planning derived from scouts in breath-holding mode has proven to be slightly more accurate and to have less variation. However, the statistically significant difference between the two automated planning methods was not found in the paired t-test (P-value 0.34).

Discussion

In this study a novel system for automated CMR planning was validated by assessing its capacity to produce accurate measurements of LV volumes, mass and function computed from the short-axis acquisitions. A number of quantitative and qualitative criteria were devised to investigate the automated CMR planning procedure and to prove its applicability in a clinical environment.

This study demonstrated good agreement in normal subjects between manual and automated CMR planning for ESV and EF for automated CMR planning derived from gated scouts in free-breathing mode and ESV, EF, and LVM for automated CMR planning derived from gated scouts in breath-holding mode. EDV was significantly different for both automated planning methods (8.05 ml mean difference for scouts in free-breathing mode; 4.22 ml for scouts in breath-holding mode). LVM measurements for automated CMR planning derived from gated scouts in free-breathing mode amount to a statistically significant mean difference of 4.72 g. The percentage of variability was low for all measurements, leading to great reliability of observed changes in parameters under consideration for both automated CMR planning methods. Bland–Altman limits of agreements were within the acceptable clinical range and corresponding plots did not reveal any systematic dependencies between

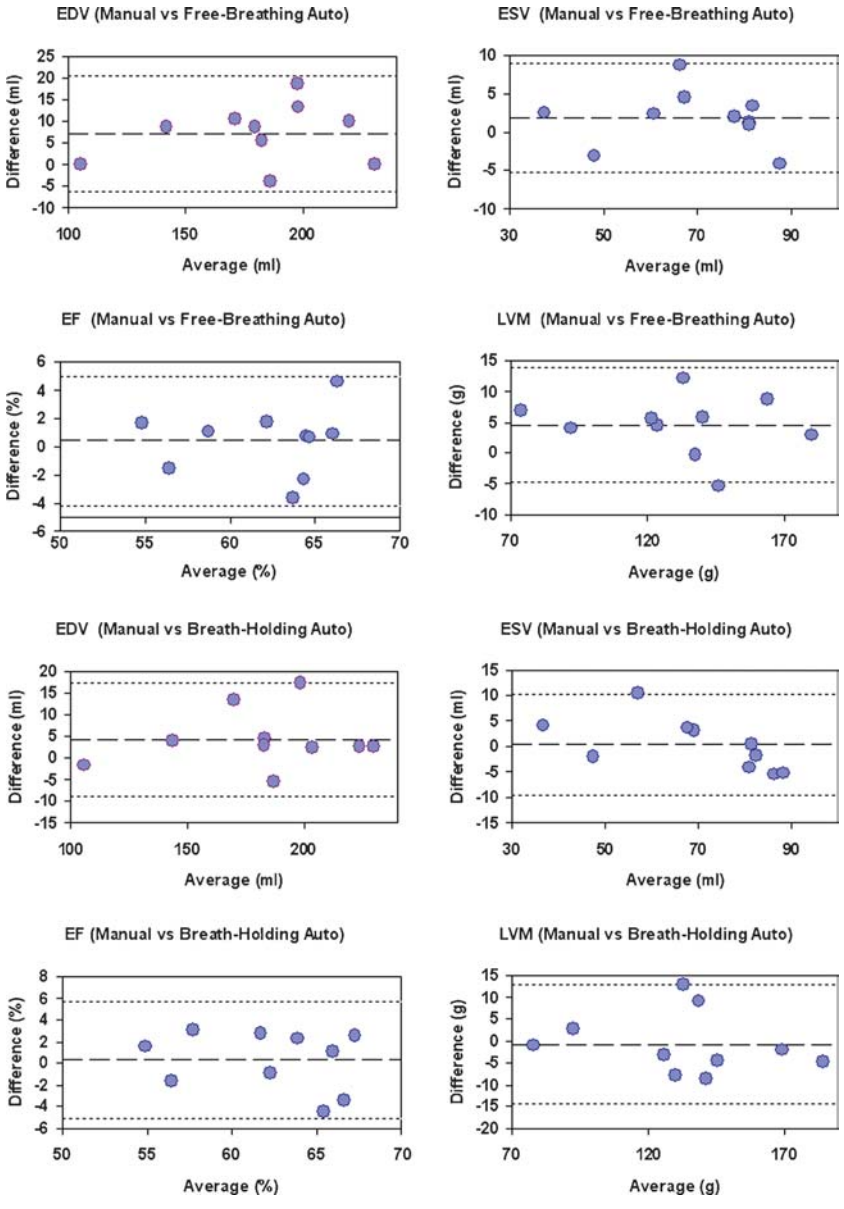

Fig. 7 Bland–Altman plots of LV volumes, mass and function for automated CMR planning derived from gated scouts in free-breathing (*two top rows*) and breath-holding (*two bottom rows*) modes compared to manual planning. The mean value and the Bland–Altman limits of agreements are shown with the dotted line

manual and automatic CMR planning methods. Thus, the automated methods for CMR planning provide accurate measurements of LV volumes, mass and function and can be utilized for these purposes in clinical routine.

The accuracy of automated CMR planning was expressed as the deviation of the imaging plane orientation. Our recent findings reported in [15] demonstrated that the intra- and inter-operator variability induced during manual CMR planning by the same operator twice and by two different operators amounted to 2.670 and 4.99° of angular LV axis deviation, respectively. The values for this particular parameter were slightly higher for both automated CMR planning (7.77° for scouts in free-breathing mode and 7.13° for scouts in breath-holding mode). According to this criterion, the accuracy of the automated CMR planning methods are closer to the inter-operator variability, while the intra-operator planning has proven to be the most consistent way of planning CMR acquisitions in terms of accuracy.

In this study, two different techniques for automated CMR planning were also compared: one based on gated scouts in free-breathing mode, the other based on gated scouts acquired at end-expiration. The total number of excellent and acceptable scores during the

visual evaluation of the system's performance amounted to 80% for automated CMR planning derived from gated scouts in breath-holding mode, while the percentage was as high as 70% for the gated scouts in free-breathing mode. Although the average LV axis deviation did not reveal statistically significant differences between the two methods, the automated CMR planning derived from gated scouts in breath-holding mode was slightly more accurate and exhibited less variation. The analysis of variability coefficients revealed that EDV and LVM showed statistically significant difference favoring automated CMR planning derived from gated scouts in breath-holding mode, while ESV and EF revealed no statistically significant difference between the automated CMR planning methods. Therefore, CMR measurements of the LV dimensions and function for automatically planned short-axis derived from gated scouts in breath-holding mode show better agreement with those from the manual planning. Thus, use of the gated scout acquisitions in breath-holding mode is a definite improvement in accuracy of automated CMR planning.

The obtained results confirmed the initial hypothesis that automated planning derived from scouts with breath-hold performs better than that from scouts in the free-breathing mode, although the disagreement between these automated methods is not significant. The small difference can be explained by the following factors. Noise introduced in the feature points describing the air-tissue boundary of the examined person due to the respiratory motion of the lungs is partially compensated by the model. Assuming that each scout image is acquired at a random phase of expiration, the model likely finds an average position between end-expiration and end-inspiration. Hence, the system for automated CMR planning demonstrated its robustness.

Automated CMR planning a is rather fast way of devising the spatial orientation of the short-axis imaging planes. Average processing times required to analyze the scout acquisition and automatically devise the orientation of SA imaging planes did not exceed 30 s on a Pentium IV 2.0 GHz computer. Up to 30 s were needed to transport the scouts via the network. The total processing time to complete automated planning amounted to 1 min. The manual planning including the time to plan 2chv and 4chv and to acquire those images sums up to 5–10 min depending on experience of the operator. Hence, the total examination time can be reduced by few minutes.

The visual assessment of our system has shown a relatively high (20–30%) failure rate. Such a high percentage of failure can be explained by the strict evaluation metrics that were utilized. Automated CMR planning was considered to be successful if the automatically planned SA stack was orthogonal to the LV axis or deviated slightly (not more than 7–8°) in at most one projection. In other words, we allowed a slight in-plane tilt of the planned SA stack in one of the LA projections. If a slight tilting was introduced in both LA projections, which still corresponds to a slight spatial deviation of the planned LV axis with respect to its true orientation, the automated planning was regarded as a failure. Considering such cases as acceptable CMR planning would decrease the overall failure rate and the expected number of successful planning would reach the 90% margin for both automated methods.

The accuracy of the LV dimension and function measurements appeared to be comparable for the manual and automated CMR planning procedures in spite of the fact that an average deviation of 7–8° for the automatically planned LV axis with respect to the true orientation was observed. The summation of the slices (Simpson's rule), which is traditionally used to compute the LV volumes, is fundamentally insensitive to the spatial orientation of the imaging planes. In a hypothetical situation with an infinite number of slices and zero slice thickness, the orientation of slices would be irrelevant. In practice, the errors in calculating cardiac volumes are due to the discrete character of measurements and incorrect identification of the endocardial and epicardial borders. Obviously, the larger the number of and thinner the slices are, the more accurate the measurements that can be obtained. However, the slice thickness and gap were kept constant for both manual and automated CMR planning procedures to reduce the discrepancy between the measurements and to justify validity of the comparison. The errors in determining the edge location in short-axis cross sections of the heart could be minimized by using the correct spatial orientation of the imaging planes. The optimal spatial orientations have been shown to be orthogonal to the intrinsic axes of the left ventricle [23, 24]. Misalignment of the imaging planes with respect to the aforementioned axes may result in blurring of the myocardial edges in the subepicardial and subendocardial areas. This phenomenon is essentially related to the in-plane image resolution being 5–6 times less than the slice thickness. Dinsmore and coauthors [23, 24] observed and reported blurring of the myocardial borders in short-axis images acquired at the oblique angle of approximately 25° and more with respect to the optimal orientation. However, the average deviation of the LV axis in this study was much less and amounted to 7–8°. Moreover, we did not observe visual differences in quality and/or appearance of short-axis images and, therefore, the impact of this factor on accuracy of the cardiac volume measurements are assumed to be negligible.

An alternative, pragmatic method to automatically plan SA acquisitions was proposed by Jackson [10], based upon the concept of the "SA scout" acquisition. The average spatial orientation of the SA imaging planes was computed from a group of adult patients and stored in the database. Instead of the traditional scout acquisitions in the transversal, coronal and sagittal directions the "SA scout" acquisition is obtained with the approximate

SA orientation. Consequently, the pseudo-SA images are automatically segmented, the left ventricular blood pool is identified, and the spatial orientation of the LV axis is found. Although acquisitions of the images in long-axis directions can be skipped and, therefore, the total examination time can be reduced, this approach suffers from one important disadvantage. The exact location and orientation of the heart inside the thoracic cavity are not known a priori and, therefore, "SA scout" acquisition is performed in more cross sections than required. This guarantees that the whole heart from the apex up to the atrioventricular ring is covered within the scanned volume, thus increasing the time to devise the location and orientation of SA imaging planes.

The same quantitative criterion was employed in [10] to assess the accuracy of the computer-aided system. The published preliminary results indicate that the mean value for the LV axis deviation amounts to 12.8°. According to this criterion, our system shows better performance and the average LV axis deviation does exceed 8°. However, the authors in [10] did not assess the impact of such a relatively large discrepancy between the manual and automatic planning procedures on the results of quantitative measurements of LV volumes, mass, and function.

Currently computer-aided systems for automated planning and CMR planning in particular are rapidly emerging on the radiological equipment market. For example, real-time planning tools are available from the manufacturers on almost all commercial MRI scanners. These real-time planning systems allow the interactive specification of the imaging planes and immediate acquisition of the images with the given spatial location and orientation. This can substantially reduce the time needed to devise the spatial orientation of the SA imaging planes and speed up the procedure of the cardiac MRI examination. However, this approach still requires permanent attention from the radiographer as well as a solid understanding of the scanned anatomy. Therefore, the real-time planning tools belong to the first generation of such systems. The automated CMR planning evaluated in this study as well as the system described in [10] may be considered second-generation tools. It allows not only rapid devising of SA cardiac acquisitions, but also hides the complexity of the planning procedure from the end user and turns CMR planning into an observer-independent routine procedure.

Limitations of the present study

Our present study was limited to normal subjects. Although the assessment of accuracy of LV volumes, mass, and function on a group of patients using automated CMR planning is highly desirable, we did not include abnormal cases. Grothues and coauthors [7] reported that sinus node dysfunction or inability of patients to withhold from breathing during the acquisition results in a lower image quality and, as a consequence, in reduced intra-, inter-observer and inter-study accuracy and reproducibility parameters in patients. These factors may negatively affect the image quality, but, in our opinion, would hardly have any effect on the accurate localization of the heart within the human thoracic cavity. On the other hand, pulmonary edema, the abnormal accumulation of extravascular fluid inside the lung parenchyma resulting from a complication of the myocardial infarction, cardiac dysfunction, and/or mitral or aortic valve diseases, changes the lung morphology and might reduce the accuracy of the automated CMR planning. The impact of this type of pathology on the accuracy of automated CMR planning deserves more attention and should be investigated in the future.

For the automated CMR planning, we used the turbo field-echo pulse scout protocol instead of the balanced FFE. The latter protocol is acquired with the dedicated cardiac coil and delivers the optimal image quality in the vicinity of the heart. Due to inhomogeneity artifacts, the tissue in the vicinity of upper lobes as well the posterior part of the lungs appear darker on the scout images and the boundary between the lungs and surrounding tissue is practically inconspicuous. Hence, the balanced FFE scout acquisition is less suitable for the automatic segmentation of the thoracic cavity, whereas the turbo field-echo pulse scout protocol is free from the aforementioned artifacts and can be easily segmented in an automatic fashion.

The system of automated CMR planning is intended to function in autonomous mode. During the prospective validation we intentionally avoided interaction with the system in order to provide comprehensive and objective analysis of its performance. Although in 80% of the cases the automated CMR planning may be performed without any interaction, the other 20% of the cases still require human supervision and manual amendment of the automatically planned short-axis imaging planes is highly desirable. However, use of our system in semi-automated mode, when the user is allowed to perform minor alterations in the orientation of the automatically planned short-axis stack, will still be beneficial and faster in comparison with the manual procedure.

Conclusions

The computer-aided system for automated planning of SA acquisition was demonstrated to be an attractive alternative to the manual procedure. This system hides the intrinsic complexity of the human heart geometry, reduces human interaction to minimum, and speeds up the process of devising the optimal location and orientation for the SA imaging planes. Combined with the predefined acquisition parameters from the scanner database, the whole

procedure of SA cardiac acquisitions can be automatically carried out. This would allow not only to provide a cost-effective solution for the assessment of the condition of the human cardiovascular system, but also to broaden the use of MRI as the imaging modality for quantification of LV volumes, ejection fraction and function.

Acknowledgements This work was supported by the Leiden University Medical Center revolving fund and the Dutch Foundation for Technical Sciences (STW, grant LPG 5651). One author (MGD) expresses his gratitude to H.C. van Assen and R.J. van der Geest for the fruitful discussion of the manuscript. We would also like to thank the anonymous reviewers for their useful comments, which undoubtedly allowed us to improve quality of the article.

References

1. Van der Wall EE, van Rugge FP, Vliegen HW, Reiber JHC, de Roos A, Bruschke AVG (1997) Ischemic heart disease: value of MR techniques. Int J Card Imaging 13:179–189
2. Sandstede JJ, Lipke C, Kenn W, Beer M, Pabst T, Hahn D (1999) Cine MR imaging after myocardial infarction-assessment and follow-up of regional and global left ventricular function. Int J Card Imaging 15:435–440
3. Darasz KH, Underwood SR, Bayliss J, Forbat SM, Keegan J, Poole-Wilson PA, Sutton GC, Pennell D (2002) Measurement of left ventricular volume after anterior myocardial infarction: comparison of magnetic resonance imaging, echocardiography, and radionuclide ventriculography. Int J Cardiovasc Imaging 18:135–142
4. Moon JCC, Lorenz CH, Francis JM, Smith GC, Pennell DJ (2002) Breath-hold FLASH and FISP cardiovascular MR imaging: left ventricular volume differences and reproducibility. Radiology 223:789–797
5. Mogelvang J, Thomsen C, Mehlsen J, Brackle G, Stubgaard M, Henriksen O (1986) Evaluation of left ventricular volumes measured by magnetic resonance imaging. Eur Heart J 7:1016–1021
6. Bogaert JG, Bosmans HT, Rademakers FE, Bellon EP, Herregods MC, Verschakelen JA, Van de Werf F, Marchal GJ (1995) Left ventricular quantification with breath hold MR imaging: comparison with echocardiography. MAGMA 3:5–12
7. Grothues F, Smith GC, Moon JCC, Bellenger NG, Collins P, Klein HU, Pennell DJ (2002) Comparison of interstudy reproducibility of cardiovascular magnetic resonance with two-dimensional echocardiography in normal subjects and in patients with heart failure or left ventricular hypertrophy. Am J Cariol 90:29–34
8. Bland JM, Altman DG (1986) Statistical Methods for assessing agreement between two methods of clinical measuments. Lancet 1:307–310
9. Lelieveldt BPF, van der Geest RJ, Lamb HJ, Kayser HWM, Reiber JHC (2001) Automated observer-independent acquisition of cardiac short axis MR images: a pilot study. Radiology 221:537–542
10. Jackson CE, Robson MD, Francis JM, Noble JA (2004) Computerized planning of the acquisition of cardiac MR images. Comput Med Imaging Graph 28:411–418
11. Gerard O, Billon AC, Rouet JM, Jacob M, Fradkin M, Allouche C (2002) Efficient model-based quantification of left ventricular function in 3-D echocardiography. IEEE Trans Med Imag 21:1059–1068
12. Ye X, Noble JA, Atkinson D (2002) 3-D freehand echocardiography for automatic left ventricle reconstruction and analysis based on multiple acoustic windows. IEEE Trans Med Imag 21:1051–1058
13. van Rossum AC, Visser FC, van Eenige MJ, Valk J, Roos JP (1987) Oblique views im magnetic resonance imaging of the heart by combined axial rotation. Acta Radiol 28:497–503
14. Lorenz CH, Walker ES, Morgan VL, Klein SS, Graham TP Jr. (1999) Normal human right and left ventricular mass, systolic function, and gender differences by cine magnetic resonance imaging. J Cardiovasc Magn Reson 1:7–21
15. Danilouchkine MG, Westenberg JJM, Reiber HJC, Lelieveldt BPF (2004) Operator induced variability in cardiovascular mr: left ventricular measurements and their reproducibility. J Cardiovasc Magn Reson (in press)
16. Lelieveldt BPF, van der Geest RJ, Rezaee MR, Bosch JG, Reiber JHC (1999) Anatomical model matching with fuzzy implicit surfaces for segmentation of thoracic colume scans. IEEE Trans Med Imaging 18:218–230
17. Lelieveldt BPF, Sonka M, Bolinger L, Scholz TD, Kayser H, van der Geest RJ, Reiber JHC (2000) Anatomical modeling with fuzzy implicit surface templates: application to automated localization of the heart and lungs in thoracic MR volumes. Comp Vis Img Understand 80:1–20
18. Pattynama PMT, Lamb HJ, van der Velde EA, van der Wall EE, de Roos A (1993) Left ventricular measurements with cine and spin-echo MR imaging: a study of reproducibility with variance component analysis. Radiology 187:261–268
19. Kayser HW, Schalij MJ, van der Wall EE, Stoel BC, de Roos A (1999) Biventricular function in patients with nonischemic right ventricle tachyarrhythmias assessed with MR imaging. Am J Roentgenol 169:995–999
20. Schala S, Nagel E, Lehmkhul H, Klein C, Bornstedt A, Schnackenburg B, Schneider U, Fleck E (2001) Comparison of magnetic resonance real-time imaging of left ventricular function with conventional magnetic resonance imaging and echocardiography. Am J Cardiol 87:95–99
21. Plein S, Smith WHT, Ridgway JP, Kassner A, Beacock DJ, Bloomer TN, Sivananthan MU (2001) Measurements of left ventricular dimensions using real-time acquisition in cardiac magnetic resonance imaging: comparison with conventional gradient echo imaging. MAGMA 13:101–108

22. Matheijssen NA, Baur LH, Reiber JH, van der Velde EA, van Dijkman PR, van der Geest RJ, de Roos A, van der Wall EE (1996) Assessment of left ventricular volume and mass by cine magnetic resonance imaging in patients with anterior myocardial infarction intra-observer and inter-observer variability on contour detection. Int J Card Imaging 12:11–19
23. Dinsmore RE, Wismer GL, Levine RA, Okada RD, Brady TJ (1984) Magnetic resonance imaging of the heart: positioning and gradient angle selection for optimal imaging planes. AJR Am J Roentgenol 143:1135–1142
24. Dinsmore RE, Wismer GL, Miller SW, Thompson R, Johnston DL, Liu P, Okada RD, Saini S, Brady TJ (1985) Magnetic resonance imaging of the heart using image planes orientated to cardiac axes – experience with 100 cases. AJR Am J Roentgenol 145:1177–1183
25. van der Geest RJ, de Roos A, van der Wall EE, Reiber JHC (1997) Quantitative analysis of cardiovascular MR images. Int J Card Imaging 13:247–258